International Journal of Pure and Applied Mathematics
Volume 115 No. 4 2017, 673-692
ISSN: 1311-8080 (printed version); ISSN: 1314-3395 (on-line version)
url: http://www.ijpam.eu
doi: 10.12732/ijpam.v115i4.3

ijpam.eu

HOMOTOPY ANALYSIS METHOD FOR ONE DIMENSIONAL UNSTEADY ADIABATIC GAS FLOW

Ruchi Bajargaan[1], Arvind Patel[2 §], Manoj Singh[3]

[1,2,3]Department of Mathematics
University of Delhi
Delhi 07, INDIA

Abstract: The approximate solution for the system of conservation laws of mass, momentum and energy governing the motion of one-dimensional unsteady adiabatic flow of a perfect gas in planar, cylindrical and spherical symmetry is obtained by applying the Homotopy analysis method (HAM) under the variable initial conditions. The 6-th order approximate values of flow variables for different values of position, time and the auxiliary parameter have been obtained and compared. The variation of flow variables have been obtained in tabular and graphical form. The existence of discontinuity or shock wave in the distribution of flow variables has been found. This approximate solution of the system of conservation laws is convergent for a range of values of position and time. The HAM solutions contain an auxiliary parameter which provides a convenient way of controlling the convergence region of series solutions. The main advantages of this method are to obtain the distribution of approximate velocity, density and pressure directly as a function of position and time which was not possible in similarity method and control the convergence region of the solution by the auxiliary parameter which is not possible in other analytic methods like variational iteration method (VIM) and adomian decomposition method (ADM).

AMS Subject Classification: 35L65, 76N15, 76M99
Key Words: homotopy analysis method, auxiliary parameter, shock wave, conservation laws

Received: September 19, 2016
Revised: June 21, 2017
Published: August 2, 2017

§Correspondence author

1. Introduction

The homotopy analysis method (HAM) was first proposed by Liao [1] in his Ph.D. thesis. A systematic and clear exposition on HAM is given in [2], [3]. In recent years, this method has been successfully employed to solve many types of nonlinear, homogeneous or nonhomogeneous, equations and systems of equations as well as problems in science and engineering. Very recently, Ahmad Bataineh et al. [4], [5] presented two modifications of HAM to solve linear and nonlinear ODEs. Abbasbandy [6], [7] presented the application of homotopy analysis method to nonlinear equations arising in heat transfer, heat radiation equations. Jafari et. al [8] obtained the solution of gas dynamic equations in two dimension for polytropic gas but the system of unsteady adiabatic flow of perfect gas in one dimension under variable initial conditions for all three symmetry by homotopy analysis method is not studied. The HAM contains a certain auxiliary parameter $\hbar$ which provides us with a simple way to adjust and control the convergence region and rate of convergence of the series solution. Moreover, by means of the so called $\hbar$-curve, it is easy to determine the valid regions of $\hbar$ to gain a convergent series solution. Homotopy analysis method avoids the need for calculating the Adomian polynomials which may be complicated. Thus, through HAM, explicit analytic solutions of nonlinear problems are possible.

In this paper, we have obtained the approximate solutions of the system of gasdynamic conservation laws governing the motion of one-dimensional unsteady adiabatic flow of a perfect gas for planar, cylindrical and spherical symmetry under the variable initial conditions by homotopy analysis method. We have obtained the distribution of approximate velocity, density and pressure directly as a function of position and time and try to control the convergence region through auxiliary parameter $\hbar$. We have computed 6-th order approximate values of flow variables for different values of position, time and the auxiliary parameter and compared those approximate values to choose proper value of $\hbar$. The variation of the flow variables with position and time is presented in form of tables and figures. We have found the existence of discontinuity or shock wave in the distribution of flow variables. All the computations are performed by using Mathematica 9.

2. Basic Ideas of Homotopy Analysis Method

We consider the following differential equations,

$$N_i[Z_i(r,t)] = 0, \quad i = 1, 2, ...n,$$

where N_i are nonlinear operators that represent the whole equations, r and t denote the independent variables and $Z_i(r,t)$ are unknown functions respectively. By means of generalizing the traditional homotopy method, Liao [2] constructed the so called zero order deformation equations

$$(1-q)L[\phi_i(r,t;q) - Z_{i,0}(r,t)] = q\hbar N_i[\phi_i(r,t;q)], \tag{1}$$

where $q \in [0,1]$ is an embedding parameter, $\hbar$ is nonzero auxiliary parameter, L is an auxiliary linear operator such that $L[f] = 0$ implies that $f = 0$ with any function f, $Z_{i,0}(r,t)$ are initial approximations of $Z_i(r,t)$ and $\phi_i(r,t,q)$ are unknown functions. It is important to note that, we have great freedom to choose auxiliary parameter $\hbar$, the initial approximations $Z_{i,0}(r,t)$ and the auxiliary linear operator L in HAM. Obviously, when $q = 0$ and $q = 1$, both

$$\phi_i(r,t;0) = Z_{i,0}(r,t) \ \text{ and } \ \phi_i(r,t;1) = Z_i(r,t),$$

hold. Thus as q increases from 0 to 1, the solutions $\phi_i(r,t;q)$ varies from the initial approximations $Z_{i,0}(r,t)$ to the solutions $Z_i(r,t)$. Expanding $\phi_i(r,t;q)$ in Taylor series with respect to q, one has

$$\phi_i(r,t;q) = Z_{i,0}(r,t) + \sum_{m=1}^{\infty} Z_{i,m}(r,t)q^m, \tag{2}$$

where

$$Z_{i,m} = \frac{1}{m!}\frac{\partial^m \phi_i(r,t;q)}{\partial q^m}\bigg|_{q=0}, \quad m = 1,2,...\infty. \tag{3}$$

If the auxiliary linear operator, the initial approximations, the auxiliary parameter $\hbar$ and the auxiliary functions are properly chosen, then the series equation (2) converges at $q = 1$ and

$$\phi_i(r,t;1) = Z_{i,0}(r,t) + \sum_{m=1}^{+\infty} Z_{i,m}(r,t),$$

which must be one of solutions of the original nonlinear equations, as proved by Liao [2]. As $\hbar = -1$, Equation (1) becomes

$$(1-q)L[\phi_i(r,t;q) - Z_{i,0}(r,t)] + qN_i[\phi_i(r,t;q)] = 0 \tag{4}$$

which are mostly used in the homotopy perturbation method [9].

According to Equation (3), the governing equations can be deduced from the zero-order deformation equations (1). Define the vectors

$$\vec{Z}_{i,n} = \{Z_{i,0}(r,t), Z_{i,1}(r,t), ...Z_{i,n}(r,t)\}$$

differentiating equation (1) m times with respect to the embedding parameter q and then setting $q = 0$ and finally dividing them by $m!$, we have the so-called mth order deformation equations

$$L[Z_{i,m}(r,t) - \chi_m Z_{i,m-1}(r,t)] = \hbar R_{i,m}(\vec{Z}_{i,m-1}), \tag{5}$$

where

$$R_{i,m}(\vec{Z}_{i,m-1}) = \frac{1}{(m-1)!} \frac{\partial^{m-1} N_i[\phi_i(r,t;q)]}{\partial q^{m-1}}\bigg|_{q=0}, \tag{6}$$

and

$$\chi_m = \begin{cases} 0, & m \leq 1 \\ 1, & m > 1. \end{cases} \tag{7}$$

It should be emphasized that $Z_{i,m}(r,t)(m \geq 1)$ is governed by the linear equation (5) with the linear boundary conditions that come from the original problem, which can be easily solved by symbolic computation softwares such as Maple and Mathematica.

3. Solution of a System of Gas Dynamic Conservation Laws

The fundamental equations governing the one-dimensional, unsteady, adiabatic flow of a perfect gas are given by [10], [11]

$$\frac{\partial \rho'}{\partial t'} + v' \frac{\partial \rho'}{\partial r'} + \rho' \frac{\partial v'}{\partial r'} + \frac{(\lambda - 1)\rho' v'}{r'} = 0, \tag{8}$$

$$\frac{\partial v'}{\partial t'} + v' \frac{\partial v'}{\partial r'} + \frac{1}{\rho'} \frac{\partial p'}{\partial r'} = 0, \tag{9}$$

$$\frac{\partial p'}{\partial t'} + v' \frac{\partial p'}{\partial r'} = \frac{\gamma p'}{\rho'} [\frac{\partial \rho'}{\partial t'} + v' \frac{\partial \rho'}{\partial r'}], \tag{10}$$

where $\lambda = 1, 2, 3$ for planar, cylindrically and spherically symmetric flow respectively; γ is the ratio of specific heats; ρ', v' and p' are fluid density, velocity and pressure at time t' and at distance r' from the plane, axis or centre of symmetry.

The initial conditions are taken as

$$\rho'(r',0) = A' e^{-\frac{r'}{\tau'}}, \quad v'(r',0) = B', \quad p'(r',0) = C' \tag{11}$$

where A', B', C' and τ' are dimensional constants.

We will change these dimensional equations and initial conditions into non-dimensional equations and initial conditions by using following transformations

$$t^{'} = t_0 t,\ r^{'} = l_0 r,\ v^{'} = v_0 v,\ \rho^{'} = \rho_0 \rho,\ p^{'} = \rho_0 {v_0}^2 p. \tag{12}$$

where t_0, l_0, v_0, ρ_0 and $\rho_0 {v_0}^2$ are characteristic time, length, velocity, density and pressure respectively.

Under the transformation in equation (12), the equations (8)-(11) reduces into non-dimensional form as

$$\frac{\partial \rho}{\partial t} + v\frac{\partial \rho}{\partial r} + \rho\frac{\partial v}{\partial r} + \frac{(\lambda - 1)\rho v}{r} = 0, \tag{13}$$

$$\delta\frac{\partial v}{\partial t} + v\frac{\partial v}{\partial r} + \frac{1}{\rho}\frac{\partial p}{\partial r} = 0, \tag{14}$$

$$\delta\frac{\partial p}{\partial t} + v\frac{\partial p}{\partial r} = \frac{\gamma p}{\rho}\left[\delta\frac{\partial \rho}{\partial t} + v\frac{\partial \rho}{\partial r}\right], \tag{15}$$

where $\delta = \frac{l_0}{v_0 t_0}$ is a Strouhal Number. This number can be used to study the extreme cases of transient and steady process.

We consider the transient process in our study, so taking Strouhal No. $\delta = 1$, the non-dimensional equations takes the form

$$\frac{\partial \rho}{\partial t} + v\frac{\partial \rho}{\partial r} + \rho\frac{\partial v}{\partial r} + \frac{(\lambda - 1)\rho v}{r} = 0, \tag{16}$$

$$\frac{\partial v}{\partial t} + v\frac{\partial v}{\partial r} + \frac{1}{\rho}\frac{\partial p}{\partial r} = 0, \tag{17}$$

$$\frac{\partial p}{\partial t} + v\frac{\partial p}{\partial r} = \frac{\gamma p}{\rho}\left[\frac{\partial \rho}{\partial t} + v\frac{\partial \rho}{\partial r}\right], \tag{18}$$

and

$$\rho(r,0) = Ae^{-\frac{r}{\tau}}, \quad u(r,0) = B, \quad p(r,0) = C. \tag{19}$$

where A, B, C and τ are non-dimensional constants.

To solve system (16)-(18) by means of homotopy analysis method (HAM), we choose the initial approximations

$$\rho_0(r,t) = Ae^{-\frac{r}{\tau}}, \quad v_0(r,t) = B, \quad p_0(r,t) = C,$$

and the linear operator

$$L[\phi_i(r,t;q)] = \frac{\partial \phi_i(r,t;q)}{\partial t}, \quad i = 1,2,3, \tag{20}$$

with the property

$$L[C_i] = 0, \tag{21}$$

where $C_i (i = 1, 2, 3)$ are integral constants and ϕ_i correspond with density, velocity and pressure for $i = 1, 2, 3$ respectively. Furthermore, systems (16), (17) and (18) suggest that we define a system of nonlinear operators as

$$\begin{aligned} N_1[\phi_i(r,t;q)] =& \frac{\partial \phi_1(r,t;q)}{\partial t} + \phi_2(r,t;q)\frac{\partial \phi_1(r,t;q)}{\partial r} \\ &+ \phi_1(r,t;q)\frac{\partial \phi_2(r,t;q)}{\partial r} + (\lambda - 1) \\ &\times \frac{\phi_1(r,t;q)\phi_2(r,t;q)}{r}, \end{aligned} \tag{22}$$

$$\begin{aligned} N_2[\phi_i(r,t;q)] =& \frac{\partial \phi_2(r,t;q)}{\partial t} + \phi_2(r,t;q)\frac{\partial \phi_2(r,t;q)}{\partial r} \\ &+ \frac{1}{\phi_1(r,t;q)}\frac{\partial \phi_3(r,t;q)}{\partial r}, \end{aligned} \tag{23}$$

$$\begin{aligned} N_3[\phi_i(r,t;q)] =& \frac{\partial \phi_3(r,t;q)}{\partial t} + \phi_2(r,t;q)\frac{\partial \phi_3(r,t;q)}{\partial r} \\ &- \gamma\frac{\phi_3(r,t;q)}{\phi_1(r,t;q)}\left[\frac{\partial \phi_1(r,t;q)}{\partial t} + \phi_2(r,t;q)\right. \\ &\left.\times \frac{\partial \phi_1(r,t;q)}{\partial r}\right]. \end{aligned} \tag{24}$$

Using the above definitions of linear operator L and non-linear operator N_i, we construct the zeroth-order deformation equations

$$(1-q)L[\phi_i(r,t;q) - Z_{i,0}(r,t)] = q\hbar N_i[\phi_i(r,t;q)], \quad i = 1, 2, 3. \tag{25}$$

Obviously, when $q = 0$ and $q = 1$,

$$\begin{aligned} &\phi_1(r,t;0) = Z_{1,0}(r,t) = \rho_0(r,t), \\ &\phi_1(r,t;1) = \rho(r,t) = Z_1(r,t), \\ &\phi_2(r,t;0) = Z_{2,0}(r,t) = v_0(r,t), \\ &\phi_2(r,t;1) = v(r,t) = Z_2(r,t), \\ &\phi_3(r,t;0) = Z_{3,0}(r,t) = p_0(r,t), \\ &\phi_3(r,t;1) = p(r,t) = Z_3(r,t). \end{aligned}$$

Therefore, as the embedding parameter q increases from 0 to 1, $\phi_i(r,t;q)$ deform from the initial approximations $Z_{i,0}(r,t)$ to the solution $Z_i(r,t)$ for i = 1, 2, 3. Expanding $\phi_i(r,t,q)$ in Taylor series with respect to q one has

$$\phi_i(r,t,q) = \phi_i(r,t,0) + \sum_{m=1}^{+\infty} \frac{1}{m!} \frac{\partial^m \phi_i(r,t;q)}{\partial q^m} q^m,$$

$$\phi_i(r,t,q) = Z_{i,0}(r,t) + \sum_{m=1}^{+\infty} Z_{i,m}(r,t) q^m,$$

where

$$Z_{i,m}(r,t) = \frac{1}{m!} \frac{\partial^m \phi_i(r,t;q)}{\partial q^m}\bigg|_{q=0}, \quad m = 1, 2, ...\infty.$$

If the auxiliary linear operator L, the initial approximations $Z_{i,0}$ and the auxiliary parameter $\hbar$ are properly chosen, the above series is convergent at $q = 1$ [2], then we have

$$\rho(r,t) = Z_{1,0}(r,t) + \sum_{m=1}^{+\infty} Z_{1,m}(r,t), \tag{26}$$

$$u(r,t) = Z_{2,0}(r,t) + \sum_{m=1}^{+\infty} Z_{2,m}(r,t), \tag{27}$$

$$p(r,t) = Z_{3,0}(r,t) + \sum_{m=1}^{+\infty} Z_{3,m}(r,t), \tag{28}$$

which must be one of the solutions of the original nonlinear equations (16), (17), (18). Now we define the vector

$$\vec{Z}_{i,n} = Z_{i,0}(r,t), Z_{i,1}(r,t), ...Z_{i,n}(r,t).$$

So the mth-order deformation equation is

$$L[Z_{i,m}(r,t) - \chi_m Z_{i,m-1}(r,t)] = \hbar R_{i,m}(\vec{Z}_{i,m-1}), \tag{29}$$

with the initial conditions

$$Z_{i,m}(r,0) = 0, \tag{30}$$

where from (22)-(24), we have

$$R_{1,m}(\vec{Z}_{i,m-1}) = (Z_{1,m-1})_t + \sum_{i=0}^{m-1} (Z_{2,i})(Z_{1,m-1-i})_r$$

$$+\sum_{i=0}^{m-1}(Z_{1,i})(Z_{2,m-1-i})_r+\frac{\lambda-1}{r}\times\sum_{i=0}^{m-1}(Z_{1,i})(Z_{2,m-1-i}),$$

$$R_{2,m}(\vec{Z}_{i,m-1})=\sum_{i=0}^{m-1}(Z_{2,m-1-i})_t+\sum_{i=0}^{m-1}\left[\sum_{j=0}^{i}(Z_{1,j})(Z_{2,i-j})\right](Z_{2,m-1-i})_r+(Z_{3,m-1})_r,$$

$$\begin{aligned}R_{3,m}(\vec{Z}_{i,m-1})=&\sum_{i=0}^{m-1}(Z_{1,i})(Z_{3,m-1-i})_t\\&+\sum_{i=0}^{m-1}\left[\sum_{j=0}^{i}(Z_{2,j})(Z_{3,i-j})\right](Z_{1,m-1-i})_r\\&-\gamma\sum_{i=0}^{m-1}(Z_{3,i})(Z_{1,m-1-i})_t\\&-\gamma\sum_{i=0}^{m-1}\left[\sum_{j=0}^{i}(Z_{2,j})(Z_{1,i-j})_r\right](Z_{3,m-1-i}).\end{aligned}$$

Now, the solution of the mth-order deformation equation (29) for $m\geq 1$ becomes

$$Z_{i,m}(r,t)=\chi_m Z_{i,m-1}(r,t)+\hbar\int_0^t R_{i,m}\vec{Z}_{i,m-1}d\tau+C_i,$$

where the integration constants $C_i(i=1,2,3)$ are determined by the initial conditions (30). Taking arbitrary constants A, B, C and τ each equal to one, we have obtained the density components

$$Z_{1,0}=e^{-r},$$

$$Z_{1,1}=\hbar t(-e^{-r}+\frac{e^{-r}(\lambda-1)}{r}),$$

$$Z_{1,2}=\hbar^2e^{-r}t(-1-\frac{1}{r}+\frac{t}{2}+\frac{t}{r^2}+\frac{t}{r}+\frac{\lambda}{r}-\frac{3t\lambda}{2r^2}$$

$$-\frac{t\lambda}{r}+\frac{t\lambda^2}{2r^2}),$$

the velocity components

$$Z_{2,0}=1,$$
$$Z_{2,1}=0,$$
$$Z_{2,2}=-\frac{1}{2}e^{-r}\hbar^2t^2\gamma$$

and the pressure components

$$Z_{3,0}=1,$$
$$Z_{3,1}=e^{-r}\hbar t\gamma,$$

$$Z_{3,2}=e^{-r}\hbar t\gamma(1+\hbar(e^{-r}+1+\frac{1}{r}-\frac{1}{2}e^{-r}t-\frac{t}{2r^2}$$
$$-\frac{t}{2r}+\frac{1}{2}e^{-r}t\gamma-\frac{\lambda}{r}+\frac{t\lambda}{2r^2}+\frac{t\lambda}{2r})).$$

Similarly, we have also obtained $Z_{1,3}$, $Z_{1,4}$, $Z_{1,5}$, $Z_{1,6}$; $Z_{2,3}$, $Z_{2,4}$, $Z_{2,5}$, $Z_{2,6}$; $Z_{3,3}$, $Z_{3,4}$, $Z_{3,5}$, $Z_{3,6}$. Then the approximate solution of $6th$ order (upto the seven components) by HAM can be given in the form

$$\rho(r,t)=Z_{1,0}+Z_{1,1}+Z_{1,2}+Z_{1,3}+Z_{1,4}+Z_{1,5}+Z_{1,6}, \tag{31}$$
$$u(r,t)=Z_{2,0}+Z_{2,1}+Z_{2,2}+Z_{2,3}+Z_{2,4}+Z_{2,5}+Z_{2,6}, \tag{32}$$
$$p(r,t)=Z_{3,0}+Z_{3,1}+Z_{3,2}+Z_{3,3}+Z_{3,4}+Z_{3,5}+Z_{3,6}. \tag{33}$$

4. Convergence of Solution

In this section, we have discussed the convergence of approximate solution for density, velocity and pressure given by Eqs. (31)-(33)in term of Liao's [2] auxiliary parameter $\hbar$. The sixth order approximate solution for density, velocity and pressure for $r=0.5$ and $t=4.0$ is plotted as function of $\hbar$ in Fig. 1(a), 1(b) and 1(c) respectively. The numerical approximate solution is computed in form of tables 1(a)-3(c) for different values of auxiliary parameter $\hbar$, postion r and time t. The figures show that the sixth order approximate solutions for planar and cylindrical symmetry are convergent for $-1.0\le\hbar\le1.0$ when $t=4$ (see

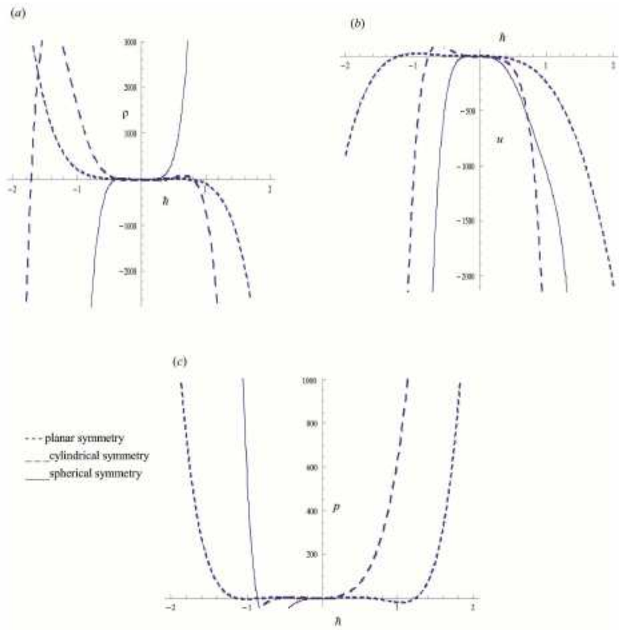

Figure 1: Distribution of flow variables (a) approximate density (b) approximate velocity (c) approximate pressure, in flow field for all the three symmetry in case of r=0.5, t=4

figs. 1(a)-1(c)) and for spherical symmetry $-1.0 \leq \hbar \leq 1.0$ when $t = 2$. This show that convergence region and rate of convergence of series solution can be controlled by auxiliary parameter $\hbar$. It is also found that with an increase in numerical value of $\hbar$, the value of approximate density, velocity and pressure increases in magnitude. Range of $\hbar$ for the convergence of approximate solution decreases as we increase the value of time t. From tables 1(a)-3(c), we found that approximate solutions are convergent for $-1.5 \leq \hbar \leq 1.0$ for all three symmetry when $r > 0$ and $0 < t \leq 2$. We also found that with increase in value of r, the approximate solution decrease for $\hbar = -1$.

5. Results and Discussion

The approximate numerical values of flow variables are calculated from Eqs. (31)-(33) for $\gamma = 1.4$, $\hbar = -1.5, -1,$
$-0.5, 1, 1.5$ and $\lambda = 1, 2, 3$ for planar, cylindrical and spherical symmetry re-

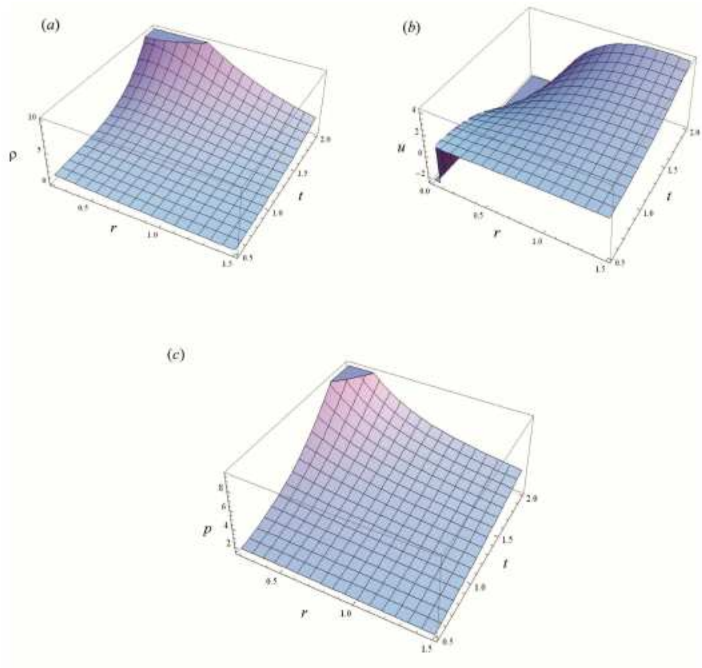

Figure 2: Distribution of flow variables (a) approximate density (b) approximate velocity (c) approximate pressure, in flow field for planar symmetry in case of $\hbar = -1$

spectively. For the each case of symmetry, the seven components of the flow variables are computed and approximate density, velocity and pressure are given in form of tables and figures. The approximate density for planar symmetry $\lambda = 1$ and $\hbar = -1$ is computed as follows

$$\begin{aligned}\rho = {} & e^{-r} + 6e^{-r}t + e^{-2r}t^3(0.3333 - 2.4e^{-r} + 0.8e^{-2r} \\ & + 3.3333e^{-3r} + \frac{3.55271 \times 10^{-15}}{r^3} - \frac{8.88178 \times 10^{-16}}{r^2} \\ & - \frac{1.77636 \times 10^{-15}}{r} + \frac{1.77636 \times 10^{-15} e^{-2r}}{r} \\ & - \frac{4.44089 \times 10^{-16} e^{-3r}}{r}) + \ldots\ldots\ldots\ldots\end{aligned}$$

The $6th$ order approximate density for $\lambda = 1$ is presented in the table 1(a) and the Fig. 2(a). Similarly, we have computed $6th$ order approximate density for $\lambda = 2$, $\lambda = 3$ for different values of r and t which are given in tables 2(a), 3(a) and Figs. 3(a), 4(a) respectively.

The $6th$ order approximate velocity for planar symmetry $\lambda = 1$ and $\hbar = -1$ is given as follows

$$\begin{aligned}
u =& 1 + e^{-r}t^2(-0.5 - 3.9e^{-r} + 5.4e^{-2r} + e^{-3r} - 3e^{-4r} \\
&+ \frac{1.77636 \times 10^{-15}}{r}) + e^{-r}t^3(1.66667 - 1.03333e^{-r} \\
&- 0.78e^{-2r} - 0.9e^{-3r} - \frac{1.77636 \times 10^{-15}e^{-2r}}{r^3} \\
&- \frac{1.42109 \times 10^{-14}e^{-r}}{r^3} - \frac{5.32907 \times 10^{-15}}{r^3} \\
&- \frac{1.77636 \times 10^{-15}e^{-3r}}{r^2} - \frac{7.10543 \times 10^{-15}e^{-r}}{r^2} \\
&- \frac{7.10543 \times 10^{-15}}{r^2} + \frac{3.55271 \times 10^{-15}e^{-3r}}{r} \\
&+ \frac{3.55271 \times 10^{-15}e^{-r}}{r} + \frac{8.88178 \times 10^{-16}}{r}) + \ldots\ldots
\end{aligned}$$

The $6th$ order approximate velocity for $\lambda = 1$, $\lambda = 2$ and $\lambda = 3$ is presented in the tables 1(b), 2(b), 3(b) and the Figs. 2(b), 3(b) and 4(b) respectively for different values of r and t.

The approximate pressure for planar symmetry $\lambda = 1$ and $\hbar = -1$ is computed as follows

$$\begin{aligned}
p = & 1 + e^{-r}t(-2.4 - e^{r} + 2.6e^{-2r} - 1.8e^{-3r} - 0.2e^{-4r} \\
&+ 0.4e^{-5r}) + e^{-r}t^2 \times (-1.77636 \times 10^{-15} + 0.4e^{-2r} \\
&- 0.96e^{-3r} + 0.16e^{-4r} + 0.4e^{-5r} - \frac{3.55271 \times 10^{-15}e^{-r}}{r^2} \\
&+ \frac{1.42109 \times 10^{-14}}{r^2} - \frac{3.55271 \times 10^{-15}e^{-3r}}{r} \\
&+ \frac{1.77636 \times 10^{-14}e^{-2r}}{r} - \frac{3.55271 \times 10^{-15}}{r}).
\end{aligned}$$

The numerical value of approximate pressure for $\lambda = 1$, $\lambda = 2$ and $\lambda = 3$ are given in the table 1(c), 2(c) and 3(c) and plotted in the Figs. 2(c), 3(c), 4(c) respectively for different values of position r and time t.

The variation of flow variables for planar symmetry $\lambda = 1$ and auxiliary parameter $\hbar = -1$ for a fixed value of time t with respect to position $r > 0$ are as follows:

(i) The approximate density decreases with respect to position $r > 0$ for any fixed value of time t(see table 1(a) and fig. 2(a)),

(ii) The approximate velocity increases very rapidly for lower values of position $r > 0$ and then gradually for any fixed value of time t (see table 1(b) and fig. 2(b)),

(iii) The approximate pressure decreases uniformly with position for any fixed value of time t (see table 1(c) and fig. 2(c)),

and variation with respect to time for a fixed value of position $r > 0$ are as follows:

(iv) The approximate density increases rapidly for lower values of r and increases gradually for higher values of r with time(see table 1(a) and fig. 2(a)),

(v) The approximate velocity decreases with time t in neighbourhood of initial point $r = 0$ and increase outside it (see table 1(b) and fig. 2(b)),

(vi) The approximate pressure increases rapidly with time for lower values of r and slowly for higher values of r.(see table 1(c) and fig. 2(c)).

Table(1a): Variation of the $6th$ order approximate density for different values of r, t and auxiliary parameter $\hbar$ for $\gamma = 1.4$ and planar symmetry $\lambda = 1$

r	t	approximate density				
		$\hbar = -1.5$	$\hbar = -1$	$\hbar = -0.5$	$\hbar = 1$	$\hbar = 1.5$
0.5	0.5	0.726576	0.999843	0.985556	-8.48253	-22.4183
	1	-1.56108	1.84475	1.58692	0.568832	41.8839
	1.5	-4.30012	4.46609	2.52149	20.1416	134.137
	2	11.5787	11.9784	3.9179	38.8923	170.209
1	0.5	0.572852	0.621112	0.596676	-5.67614	-17.3637
	1	1.00064	1.20378	0.950942	-2.8129	4.70169
	1.5	4.17624	2.69469	1.48036	4.72684	38.0427
	2	17.6493	6.12495	2.23646	12.1797	51.6833
1.5	0.5	0.379692	0.376298	0.361491	-3.57164	-11.384
	1	0.88	0.704225	0.573055	-2.4504	-1.60372
	1.5	2.93001	1.43893	0.884239	1.18001	14.5978
	2	9.24081	2.93731	1.32271	5.02333	23.6505

Table(1b): Variation of the 6-th order approximate value of velocity for different values of r, t and auxiliary parameter $\hbar$ with $\gamma = 1.4$ and planar symmetry $\lambda = 1$

r	t	approximate velocity				
		$\hbar = -1.5$	$\hbar = -1$	$\hbar = -0.5$	$\hbar = 1$	$\hbar = 1.5$
0.5	0.5	0.951942	1.03057	1.04962	-10.5768	-60.9243
	1	-0.202914	1.0534	1.21546	-38.2219	-197.207
	1.5	-5.23756	1.07146	1.52837	-73.5297	-352.551
	2	-17.2175	1.31576	2.02607	-110.76	-493.928
1	0.5	1.0488	1.12831	1.03725	-3.8275	-22.8501
	1	0.981189	1.57319	1.15759	-15.453	-75.5963
	1.5	0.398	2.47213	1.37419	-30.3573	-135.29
	2	-1.05934	4.0278	1.70004	-45.9756	-187.684
1.5	0.5	1.20246	1.13563	1.02467	-1.29874	-9.76179
	1	1.88044	1.60671	1.10292	-6.84409	-33.5169
	1.5	3.18324	2.53055	1.24062	-13.9476	-60.1519
	2	5.34452	4.05	1.44276	-21.3452	-82.8851

Table(1c): Variation of the 6-th order approximate pressure for different values of r, t and auxiliary parameter $\hbar$ with $\gamma = 1.4$ and planar symmetry $\lambda = 1$

r	t	approximate pressure				
		$\hbar = -1.5$	$\hbar = -1$	$\hbar = -0.5$	$\hbar = 1$	$\hbar = 1.5$
0.5	0.5	1.58298	1.66072	1.37642	34.1332	135.632
	1	4.91886	2.93173	1.83168	47.7695	157.955
	1.5	18.177	5.18968	2.35515	43.5902	84.5937
	2	47.9768	8.42326	2.92412	26.5147	-40.8427
1	0.5	1.71116	1.56062	1.26686	16.127	58.3158
	1	3.7646	2.44903	1.59144	21.1597	61.9241
	1.5	8.70653	3.73404	1.97214	18.2342	27.7248
	2	16.9116	5.30866	2.40407	10.2102	-22.7231
1.5	0.5	1.59422	1.42867	1.17752	8.77195	29.3374
	1	2.81059	2.06637	1.39486	10.989	29.4236
	1.5	5.01887	2.9509	1.65339	9.19794	11.8611
	2	8.04516	4.06169	1.95358	5.02473	-12.2455

The variation of flow variables for cylindrical symmetry $\lambda = 2$ and auxiliary parameter $\hbar = -1$, for a fixed value of t with respect to position $r > 0$ are as follows:

(i) The approximate density firstly increases and then decreases with respect to position $r > 0$ (see table 2(a) and fig. 3(a)),

(ii) The approximate velocity increases uniformly with respect to position for all values of t and there exist shock wave in the neighbourhood of $r = 0$ (see table 2(b) and fig. 3(b)),

(iii) The approximate pressure increases uniformly with respect to position for all values of t(see table 2(c) and fig. 4(c)),

and variation with respect to time for a fixed value of position $r > 0$ are as follows:

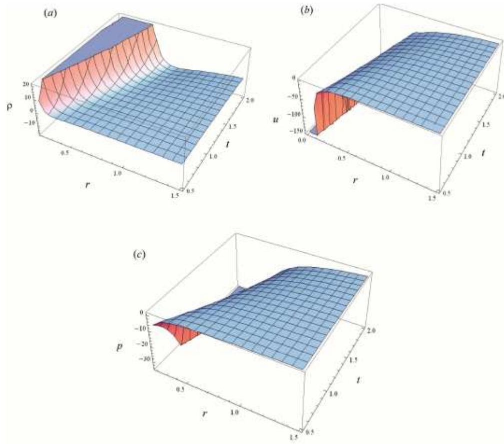

Figure 3: Distribution of flow variables (a) approximate density (b) approximate velocity (c) approximate pressure, in flow field for cylindrical symmetry in case of $\hbar = -1$

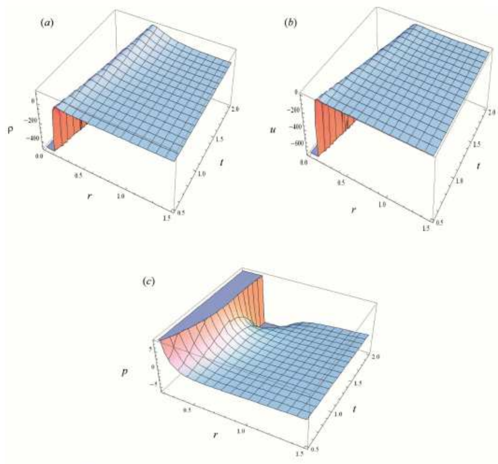

Figure 4: Distribution of flow variables (a) approximate density (b) approximate velocity (c) approximate pressure, in flow field for spherical symmetry in case of $\hbar = -1$

(iv) The approximate density increases with time for $r < 1$ and then decreases with time for $r > 1$ (see table 2(a) and fig. 3(a)),

(v) The approximate velocity decreases with time for $r > 0$ (see table 2(b) and fig. 3(b)),

(vi) The approximate pressure decreases with time for $r > 0$ (see table 2(c) and fig. 4(b)).

Table(2a): Variation of the 6-th order approximate density for different values of r, t and the auxiliary parameter $\hbar$ with $\gamma = 1.4$ and cylindrical symmetry $\lambda = 2$

r	t	approximate density				
		$\hbar = -1.5$	$\hbar = -1$	$\hbar = -0.5$	$\hbar = 1$	$\hbar = 1.5$
0.5	0.5	1.18904	-0.230519	-0.006882	-8.9825	-72.5218
	1	32.2053	-1.20643	-1.54942	-53.2625	-288.037
	1.5	201.864	8.71598	-3.8791	-71.0108	-220.607
	2	680.6	58.0432	-5.6761	-0.839081	485.931
1	0.5	0.256212	0.248833	0.307891	-4.2856	-21.4344
	1	-0.684341	-0.524845	0.0447471	-12.8597	-54.4885
	1.5	-4.63733	-2.73737	-0.553049	-17.471	-51.82
	2	-14.5898	-7.03151	-1.60752	-11.7953	19.828
1.5	0.5	0.217578	0.233241	0.246464	-2.8469	-11.9177
	1	-0.197155	0.0780395	0.219568	-5.7169	-20.6842
	1.5	-2.05853	-0.498015	0.990336	-6.4867	-16.0111
	2	-7.01433	-1.84133	-0.167849	-4.1045	5.80495

Table(2b): Variation of the 6-th order approximate velocity for different values of r, t and the auxiliary parameter $\hbar$ with $\gamma = 1.4$ and cylindrical symmetry $\lambda = 2$

r	t	approximate velocity				
		$\hbar = -1.5$	$\hbar = -1$	$\hbar = -0.5$	$\hbar = 1$	$\hbar = 1.5$
0.5	0.5	-3.49833	-1.11199	0.427618	17.855	81.506
	1	-28.8075	-10.8033	1.28747	4.48001	-63.9751
	1.5	-66.0846	-27.1953	-3.43289	-78.7435	-606.807
	2	-141.306	-42.8949	-4.14705	-226.536	-1461.7
1	0.5	0.213538	0.545193	0.882449	1.84775	4.69784
	1	-4.18808	-1.40948	0.509332	-2.0796	-22.7798
	1.5	-15.9129	-5.77956	-0.122366	-16.3706	-108.439
	2	-38.5516	-13.2366	-0.965009	-42.0297	-246.21
1.5	0.5	0.711171	0.85899	0.963807	0.408339	-10.83661
	1	-0.743941	0.277173	0.848174	-2.45288	-16.5928
	1.5	-4.6734	-1.02655	0.646492	-8.436841	-46.8434
	2	-12.9295	-3.3549	0.35959	-17.5281	-89.9471

Table(2c): Variation of the 6-th order approximate pressure for different values of r, t and the auxiliary parameter $\hbar$ with $\gamma = 1.4$ and cylindrical symmetry $\lambda = 2$

r	t	approximate pressure				
		$\hbar = -1.5$	$\hbar = -1$	$\hbar = -0.5$	$\hbar = 1$	$\hbar = 1.5$
0.5	0.5	-0.969907	-0.480348	0.270705	2.76717	38.0653
	1	-20.0171	-5.02217	-0.54647	58.3423	346.992
	1.5	-91.5485	-15.0579	-1.33398	135.295	703.189
	2	-251.377	-32.0715	-1.84027	207.931	925.601
1	0.5	0.440517	0.658884	0.831076	7.73155	33.0307
	1	-2.33441	-0.240285	0.603708	20.7151	91.9993
	1.5	-9.32252	-1.97802	0.325294	33.1002	134.349
	2	-20.7932	-4.63662	0.0166979	39.2662	126.084
1.5	0.5	0.91442	0.960831	0.974211	5.80598	20.9433
	1	0.304042	0.746874	0.924776	10.7861	39.8511
	1.5	-1.21934	0.250222	0.851149	14.1695	47.1042
	2	-3.84253	-0.623969	0.756163	14.7681	36.6136

Table(3a): Variation of the 6-th order approximate density for different values of r, t and the auxiliary parameter $\hbar$ with $\gamma = 1.4$ and spherical symmetry $\lambda = 3$

r	t	approximate density				
		$\hbar = -1.5$	$\hbar = -1$	$\hbar = -0.5$	$\hbar = 1$	$\hbar = 1.5$
0.5	0.5	-0.758977	0.79676	-0.0759664	40.8797	86.7307
	1	41.0756	15.0516	0.839668	-27.3953	-593.682
	1.5	277.409	65.0556	5.66841	-184.253	-1729.85
	2	545.355	118.99	15.5598	-166.008	-1068.16
1	0.5	0.267873	1.150206	0.146378	4.55563	6.04436
	1	3.79589	0.396332	-0.113222	-9.20661	-85.681
	1.5	25.0406	3.17108	-0.253428	-39.1913	-255.521
	2	88.1843	12.0344	0.002733	-75.019	-419.748
1.5	0.5	0.155795	0.151964	0.164399	-0.13528	-4.00715
	1	0.251675	0.0050073	0.0547606	-5.11735	-29.815
	1.5	1.6076	0.0870796	-0.103372	-12.8054	-64.3838
	2	6.54361	0.267574	-0.287448	-20.5285	-89.9351

Table(3b): Variation of the 6-th order approximate velocity for different values of r, t and the auxiliary parameter $\hbar$ with $\gamma = 1.4$ and spherical symmetry $\lambda = 3$

r	t	approximate velocity				
		$\hbar = -1.5$	$\hbar = -1$	$\hbar = -0.5$	$\hbar = 1$	$\hbar = 1.5$
0.5	0.5	-4.90507	-1.16878	0.092457	64.5023	349.465
	1	-21.3402	-0.837753	-1.63988	106.682	391.446
	1.5	-6.73899	11.7883	-2.93711	-77.1352	-1199.75
	2	-249.258	-13.8429	-4.99894	-570.732	-4704.23
1	0.5	-0.243178	0.185651	0.757552	9.40197	45.195
	1	-4.07215	-2.07368	0.103024	21.4925	95.1623
	1.5	-5.30057	-4.78316	-0.82191	18.3252	32.3669
	2	9.23376	-6.38433	-1.86057	-15.6464	-232.212
1.5	0.5	0.34922	0.641317	0.909903	2.49819	8.67677
	1	-1.83516	-0.48242	0.64994	4.24861	15.08
	1.5	-5.29648	-2.35246	0.242815	2.65117	-0.8924
	2	-8.68264	-4.83335	-0.280577	-5.03533	-53.6112

Table(3c): Variation of the 6-th order approximate pressure for different values of r, t and the auxiliary parameter $\hbar$ with $\gamma = 1.4$ and spherical symmetry $\lambda = 3$

r	t	approximate pressure				
		$\hbar = -1.5$	$\hbar = -1$	$\hbar = -0.5$	$\hbar = 1$	$\hbar = 1.5$
0.5	0.5	6.74928	0.0472244	-0.132784	-73.4914	-301.221
	1	54.68	1.55515	-0.530309	-3.7107	274.046
	1.5	148.7	0.513855	-0.993699	312.499	2417.47
	2	288.569	-15.268	-2.756	1010.99	7126.01
1	0.5	0.304645	0.250432	0.527773	-7.5942	-28.8694
	1	0.0797088	-0.386268	0.15054	4.16475	51.0505
	1.5	-1.12823	-0.978408	-0.142549	34.5745	226.279
	2	-8.22921	-1.88178	-0.384029	78.6787	456.354
1.5	0.5	0.542639	0.64537	0.810105	1.02209	3.10163
	1	-0.217803	0.215145	0.621045	6.13812	30.7484
	1.5	-1.44653	-0.282716	0.438554	14.4416	71.3544
	2	-3.12013	-0.824169	0.266512	23.7117	110.012

The variation of flow variables for spherical symmetry $\lambda = 3$ and auxiliary parameter $\hbar = -1$, for a fixed value of t with respect to position $r > 0$ are as follows:

(i) The approximate density has sudden discontinuity with respect to position r in neighbourhood of $r = 0$ for any fixed time t. After discontinuity, the density decreases with position rapidly for all values of time t(see table 3(a) and fig. 4(a)),

(ii) The approximate velocity generally increases with position r for fixed value of time t (see table 3(b) and fig. 4(b)),

(iii) The approximate pressure generally increases with position for fixed value of time t (see table 3(c) and fig. 4(c)),

and variation of flow variables with respect to time for a fixed value of $r > 0$, is as follows

(iv) With time t, the approximate density increases rapidly for lower values of position $r < 1$ but slowly for higher values of position $r > 1$(see table 3(a) and fig. 4(a)),

(v) With time t, the approximate velocity decreases with position r(see table 3(b) and fig. 4(b)),

(vi) With time t, the approximate pressure decreases for all values of position $r > 0$ except in region $0 < r < 0.8$ and $1.5 < t < 2$(see table 3(c) and fig. 4(c)).

The above variations show the existence of shock wave in the distribution of velocity, density and pressure with respect to position(see figs. 2, 3, 4). The main advantages of this method are to obtain the distribution of approximate velocity, density and pressure directly as a function of position and time which is not possible in similarity method and control the convergence region which is not possible in other analytic methods like VIM and ADM.

6. Conclusions

In present work, it is shown that the homotopy analysis method can be applied successfully for the solution of the system of gasdynamic conservation laws governing the motion of one-dimensional unsteady adiabatic flow of a perfect gas under the variable initial conditions for all the three types of symmetry. On the basis of this work, one may draw the following conclusions:

(i) The existence of discontinuities or shock waves in the distribution of flow variables have been found. In planar symmetry, approximate velocity has discontinuity at r=0. In cylindrical and spherical symmetry, the positions of discontinuities in approximate density, approximate velocity and approximate pressure can be identified.

(ii) The range of $\hbar$ for the convergence of approximate solution decreases as we increase the value of time t. The valid region of auxiliary parameter for the convergence of solution in case of planar and cylindrical symmetry is $-1 \leq \hbar \leq 1$ when $t = 4$ and for spherical symmetry is $-1 \leq \hbar \leq 1$ when $t = 2$.

(iii) The convergence of approximate solution for density, velocity and pressure can be controlled by auxiliary parameter.

(iv) The flow variables have different variations in different symmetries.

(v) This work show that the homotopy analysis method can be used in study of more realistic gasdynamic problems.

Acknowledgments

The research of the author (Ruchi Bajargaan) is supported by CSIR, New Delhi, India vide letter no. 09/045(1264)/2012-EMR-I. The second author

(Arvind Patel) thanks to the University of Delhi, Delhi, India for the R&D grant vide letter no. RC/2014/6820 dated oct. 15, 2014. The third author (Manoj Singh) is supported by UGC, New Delhi, India vide letter no. Sch. No./JRF/AA/139/F-297/2012-13 dated January 22, 2013.

References

[1] S.J. Liao, *The Proposed Homotopy Analysis Techniques for the Solution of Nonlinear Problems*, Ph.D. dissertation, Shanghai Jiao Tong University, Shanghai, 1992.

[2] S.J. Liao, *Beyond Perturbation: Introduction to the Homotopy Analysis Method*, CRC Press, Chapman and Hall, Boca Raton, 2003.

[3] S.J. Liao, Notes on the homotopy analysis method: Some definitions and theorems, *Communications in Nonlinear Science and Numerical Simulation*, **14** (2009), 983-997, **doi:** 10.1016/j.cnsns.2008.04.013.

[4] A. Sami Bataineh, M.S.M. Noorani, I. Hashim, On a new reliable modification of homotopy analysis method, *Communications in Nonlinear Science and Numerical Simulations*, **14** (2009), 409-423, **doi:** 10.016/j.cnsns.2007.10.007.

[5] A. Sami Bataineh, M.S.M. Noorani, I. Hashim, Modified homotopy analysis method for solving systems of second-order BVPs, *Communications in Nonlinear Science and Numerical Simulations*, **14** (2009), 430-442, **doi:** 10.016/j.cnsns.2007.09.012.

[6] S. Abbasbandy, The application of homotopy analysis method to nonlinear equations arising in heat transfer, *Phys Lett A*, **360** (2006), 109-113, **doi:** 10.1016/j.physleta.2006.07.065.

[7] S. Abbasbandy, Homotopy analysis method for heat radiation equations, *International Communications in Heat and Mass Transfer*, **34** (2007), 380-387, **doi:** 10.1016/j.icheatmasstransfer.2006.12.001.

[8] H. Jafari, C. Chun, S. Seifi, M. Saeidy, Analytical solution for nonlinear gas dynamic equation by homotopy analysis method, *Applications and Applied Mathematics*, **4**, No. 1 (2009), 149-154.

[9] J.H. He, Homotopy perturbation method: A new nonlinear analytical technique, *Applied Mathematics and Computation*, **135** (2003), 73-79.

[10] L.I. Sedov, *Similarity and Dimensional Methods in Mechanics*, Academic Press, New York, 1959.

[11] J.P. Vishwakarma, Propagation of shock waves in a dusty gas with exponentially varying density, *Eur. Phys. J. B*, **16** (2006), 369-372, **doi:** 10.1007/s100510070238.